

Infrared and Raman studies on $a\text{-Ge}_{1-x}\text{Sn}_x\text{:H}$ thin films

E. Ching-Prado, R. S. Katiyar, W. Muñoz, O. Resto, and S. Z. Weisz

Department of Physics, University of Puerto Rico, Box 23343, San Juan, Puerto Rico 00931

(Received 20 January 1994)

Infrared and Raman measurements were carried out on $a\text{-Ge}_{1-x}\text{Sn}_x\text{:H}$ thin films grown on Si substrates. The hydrogen concentration is found to decrease with increasing tin content. Preferential formation of monohydride groups (GeH) is observed with increasing Sn concentration. The tin dependence of the GeH and GeH_2 stretching is explained as being due to the lower electronegativity of Sn in comparison to that of Ge. The study reveals that the stability-ratio electronegativity of germanium should be smaller than 3.59 for the $a\text{-Ge:H}$ system. Also, the GeH wagging and GeH_2 roll modes show that there is a large bond-angle variation with increasing Sn concentration. Additionally, the changes in the frequency, width, and intensity of the Ge-Ge (TO)-like phonon, clearly indicate that the structural disorder increases with increasing tin content. Auger-electron microprobe and Raman studies with different excitation laser lines show differences near the surface in comparison to the bulk, which are produced by the partial segregation of tin atoms, formation of Sn clusters in the surface, and reduction of the germanium concentration near the surface, as well as preferential attachment of hydrogen to Ge rather than to Sn.

INTRODUCTION

During the past few years amorphous hydrogenated silicon and germanium have been employed in several optoelectronic applications, such as solar cell, photosensors, and thin-film transistors.^{1,2} The addition of tin into silicon and germanium has been found to decrease the optical band gap systematically with increasing Sn concentration, thereby allowing one to control the electrical and optical properties of such alloys over a wide composition range.³

Amorphous hydrogenated germanium ($a\text{-Ge:H}$) has been prepared by different techniques, such as sputtering and glow discharge.¹⁻⁴ However, the vibrational spectrum of this material has not been studied as extensively as that of $a\text{-Si:H}$. Most of the conclusions on $a\text{-Ge:H}$ from the infrared and Raman spectra have been drawn by comparison with $a\text{-Si:H}$ and by studies involving substitution of hydrogen by deuterium.^{5,6} The vibrational spectrum of alloy systems involving Ge (or Si), H, and Sn have been studied very little.^{3,7,8} On the other hand, $a\text{-Si}_{1-x}\text{Ge}_x\text{:H}$ is the alloy material that has received most of the attention.^{9,10} X-ray diffraction experiments on the unhydrogenated $a\text{-Ge}_{1-x}\text{Sn}_x$ system were carried out by Temkin, Conell, and Paul,¹¹ on samples grown at -10°C . They had reported random covalent bonding in them. Also, Oguz and Paul¹² studied the synthesis of metastable crystalline Ge-Sn alloys by pulsed UV laser annealing of amorphous Ge-Sn films. Raman scattering in $a\text{-Sn}_{1-x}\text{Ge}_x$ alloys was investigated by Menéndez *et al.*,¹³ where differences with the $\text{Ge}_{1-x}\text{Si}_x$ system were understood considering confinement and strain effects. Chambouleyron and Marques¹⁴ have studied transport and optical properties of hydrogenated and unhydrogenated germanium tin alloys grown at a higher deposition temperature (180°C). However, their infrared study was aimed

simply at identifying hydrogen bonds as well as its concentration. A previous work by Chambouleyron and Marques¹⁵ on the same hydrogenated material reported that the position of the infrared bands appears slightly shifted toward low frequencies as in the tin concentration increases.

In this work we present a detailed vibrational study of $a\text{-Ge}_{1-x}\text{Sn}_x\text{:H}$ as a function of tin contents. The Ge-Ge (TO)-like phonon was studied by means of Raman scattering, while infrared spectroscopy was employed to measure Ge-H and Ge-H_2 modes.

EXPERIMENT

Two sets of $a\text{-Ge}_{1-x}\text{Sn}_x\text{:H}$ films were prepared on Si substrates in a conventional reactive cosputtering unit with 150 W of RF (13.56 MHz) power, a cathode self-bias voltage of -1000 V, and a gas mixture of argon at 12 mTorr and hydrogen at 3 mTorr. The sputtering target consisted of a germanium disk of about 15 cm in diameter and a couple of tin pieces (about 1 cm in diameter) placed at one end of the germanium disk. The substrates were heated to about 150°C during the deposition. The usual deposition time was about six hours. Characterization of the films was carried out using Auger electron microprobe. We used depth profiling to determine the uniformity of the composition of the film throughout the sample thickness. X-ray diffraction was employed to detect any crystalline inclusion in the samples, such as $\beta\text{-Sn}$. The first set corresponds to samples *A*, *B*, *C*, and *D* [see Table I(a)]. A second set similar to the first one, but with slightly different tin content, was prepared. The samples of this set are called 1, 2, 3, and 4 [see Table I(b)]. In order to carry out infrared absorption studies we utilized a Nicolet 740 Fourier transform infrared spectrometer (FTIR). The parameters were chosen to give a

TABLE I. (a) Composition and refractive index of the first set of samples. (b) Composition and refractive index of the second set of samples.

(a)			
Sample	X (%)	Refrac. index	N_H (%) ^a
A	6.9	4.3	6.4
B	4.5	4.1	7.3
C	1.0	3.6	7.6
D	0.4	3.0	6.9
(b)			
Sample	X (%)	Refrac. index	N_H (%) ^a
1	7.6	5.0	5.6
2	5.9		
3	2.6		
4	0.7	3.4	7.1

^aRelative to crystalline Ge.

resolution of 4 cm^{-1} in the range 4000 to 400 cm^{-1} . Raman spectra were collected using a Raman Microprobe S3000 system, from Instruments S.A, equipped with a diode array from Princeton Instruments as the detection system. The excitation sources were the 514.5 nm laser radiation from an argon ion laser, INNOVA 90-6, and the 581 - and 588-nm lines from a CR-599 dye laser, both from Coherent Inc. The spectra were measured in the backscattering geometry with a $100\times$ microscope objective. A defocused laser spot was used in order to avoid recrystallization (by laser annealing effect) or degradation of the films.

RESULTS AND DISCUSSION

A. Infrared absorption

Table I presents the stoichiometric data obtained from the Auger electron spectroscopy study. Except for a surface layer of a few angstroms, the composition of the film was found to be quite uniform. Tin segregation was observed in the samples, with the highest tin concentration near the surface being between 1.7 (sample D) and 2.4 (sample 1) times higher than that in the bulk. No evidence of crystalline structure was found from x-ray diffraction measurements. All the samples were found to contain carbon, with a lower concentration in the bulk than in the surface. Figure 1 shows typical infrared spectra obtained with $a\text{-Ge}_{1-x}\text{Sn}_x\text{:H}$. The bands around 1880 and 1970 cm^{-1} were assigned to stretching modes of GeH and GeH₂ groups, respectively.^{1,16} Also, a band around 570 cm^{-1} is indicative of wagging-roll modes of these groups.¹⁶ No infrared signal from Sn-H bonds was found, which might be due to the low Sn concentration and a preferential attachment of hydrogen to germanium rather than to tin.¹⁴ A preferential attachment was also observed in $a\text{-Si}_{1-x}\text{Sn}_x$ by Katiyar *et al.*¹⁷ Evidence of preferential hydrogen attachment has been reported in other systems, such as $a\text{-Si}_{1-x}\text{Ge}_x\text{:H}$, where hydrogen prefers to attach to Si than to Ge.^{10,18,19} In these cases the wagging-roll modes were used in order to estimate the hydrogen concentration in the samples,¹⁶ whose value de-

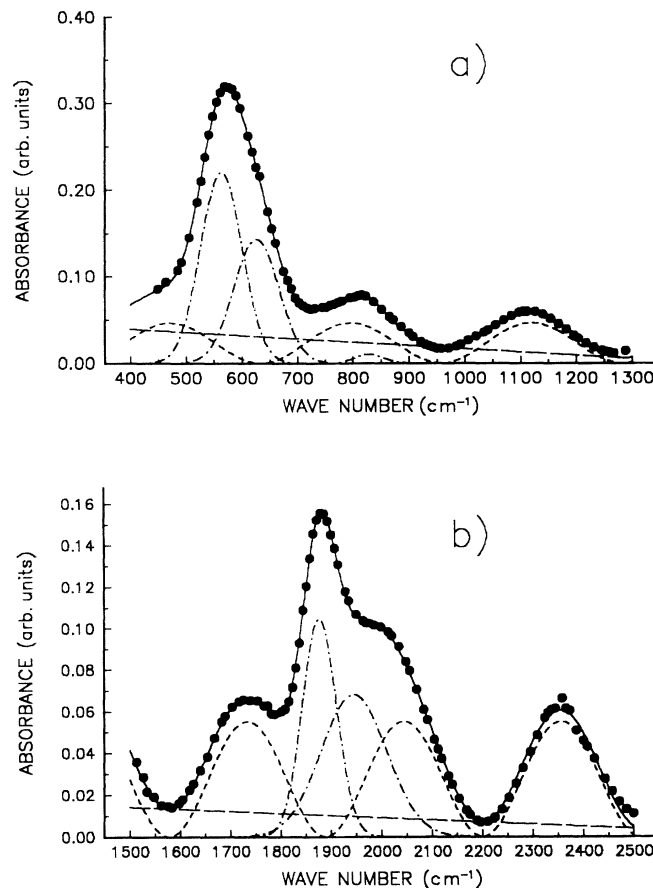


FIG. 1. Absorbance spectra of $a\text{-Ge}_{1-x}\text{Sn}_x\text{:H}$ for (a) GeH and GeH₂ bending modes, and (b) GeH and GeH₂ stretching modes with x between 0.4% and 7.6% . Dot-dashed lines correspond to absorption bands, short-dashed lines to fringes, and long-dashed lines to background.

creases with increasing Sn content (see Table I). The absorption band and the fringes were fitted using Gaussian and sine squared functions, respectively. From the fringes the refractive indices were calculated, which are reported in Table I. The absorption coefficients were calculated using the approximation suggested by Brodsky, Cardona, and Cuomo.²⁰ The spectra of the stretching modes are shown in Fig. 2 for different x values. Several changes are found as the Sn concentration increases. There is a systematic decrease in the intensity of the GeH₂ mode, while the intensity of the GeH stretching mode increases. This is associated with the preferential formation of GeH instead of GeH₂ bonds. This behavior was also found in the $a\text{-Si}_{1-x}\text{Sn}_x$ system.¹⁷ Moreover, the decrease in intensity of the band around 825 cm^{-1} , associated with the scissors mode of the GeH₂ group, with increasing Sn content confirms the preferential formation of the GeH group.

Figure 3 shows the deconvoluted band around 570 cm^{-1} , where two Gaussian functions were necessary in order to fit the spectra. Clearly, the intensity of the Gaussian peak around 620 cm^{-1} has the same evolution as the stretching mode of GeH₂ group with respect to Sn concentration. A similar behavior is observed for the

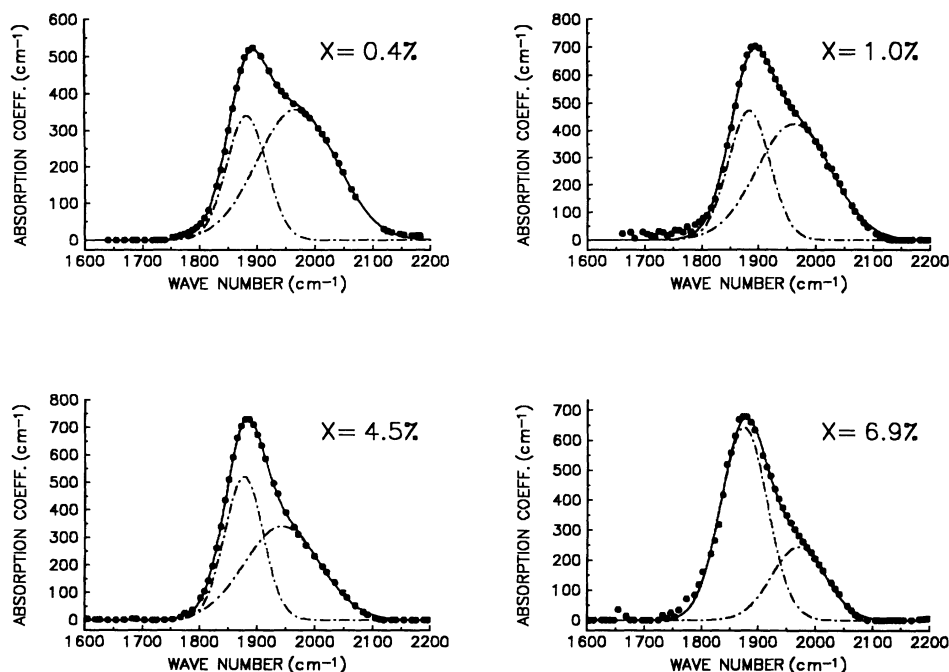


FIG. 2. Absorption coefficient vs frequency for the GeH and GeH_2 stretching modes of $a\text{-Ge}_{1-x}\text{Sn}_x\text{:H}$ with $x=0.4\%$, 1.0% , 4.5% , and 6.9% . Dot-dashed lines correspond to absorption bands.

Gaussian peak around 565 cm^{-1} and the stretching mode of the GeH group. These results suggest that the peak around 565 cm^{-1} corresponds to the GeH wagging mode, while the peak around 620 cm^{-1} corresponds to the GeH_2 roll mode. Connell and Pawlik²¹ found that the band around 570 cm^{-1} in $a\text{-Ge:H}$, prepared by sputtering technique is asymmetric. This asymmetry varies in samples prepared under different hydrogen pressures. Thus, the deconvolution of their data shows peaks at 564.5 cm^{-1} (0.07 eV) and 625.1 cm^{-1} (0.0775 eV), in good agreement with our results. Despite the conclusion about

the band at 1976 cm^{-1} (later reported by Lucovsky, Nemanich, and Knights²² to arise from GeH_2 rather than GeH) Connell and Pawlik²¹ indicated that the hydrogen incorporation results in the two final-state configurations that have different excitation energies for stretching and angular modes. Moreover, Bermejo and Cardona²³ studied $a\text{-Ge:H}$, by infrared spectroscopy, showing an asymmetric wagging mode, where in some cases (for different hydrogen partial pressures) a shoulder around 620 cm^{-1} was found. These results are also consistent when compared with the experimental values of hydrogen adsorbed

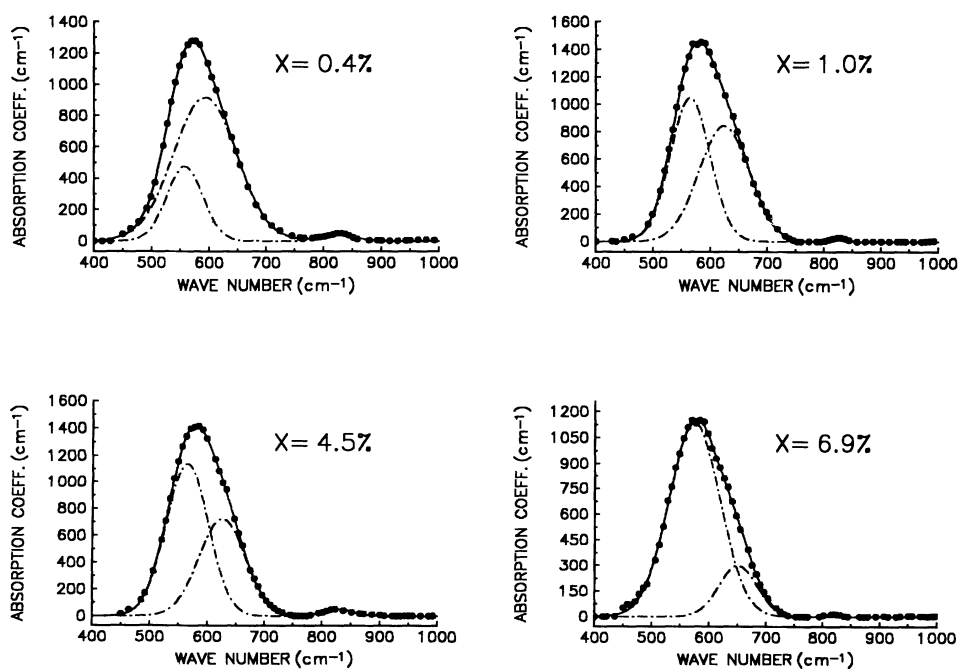


FIG. 3. Absorption coefficient vs frequency for the GeH and GeH_2 bending modes of $a\text{-Ge}_{1-x}\text{Sn}_x\text{:H}$ with $x=0.4\%$, 1.0% , 4.5% , and 6.9% . Dot-dashed lines correspond to absorption bands.

on (111) Si surfaces and with the $(\text{SiH}_2)_m$ system, m being equal to 5 and 6. In the former the SiH wagging mode is found at around 630 cm^{-1} , while in the latter the SiH₂ roll mode can be found between 625 and 720 cm^{-1} . Furthermore, it has been mentioned that the roll mode may occur at a higher frequency than the wagging mode.¹⁶ We will return to this point later.

Figure 4 presents the evolution of the GeH and GeH₂ stretching modes as a function of tin concentration. A trend toward lower frequencies is observed as the Sn content increases. An explanation for this behavior can be obtained through an analysis of the nature of the R^i nearest neighbor associated with the Ge atom that participates in the Ge-H stretching modes. This kind of analysis has been applied by Lucovsky and co-workers^{22,24} to the case of silicon. Figure 5 shows the frequency of the Si-H and Ge-H stretching modes with respect to the sum of stability ratio electronegativities ($\sum SR^i$) (Ref. 25) of substituted silane and germane ($RR'R''XH$, where $X = \text{Si}$ or Ge and $R^i = \text{F}, \text{Cl}, \text{Br}, \text{CH}_3, \text{C}_2\text{H}_5$, etc.)²⁴⁻³² A shift to lower frequencies can be observed as $\sum SR^i$ decreases. Similar results are found in $RR'XH_2$ (Fig. 6). Thus, the decreasing of the Ge-H stretching modes in hydrogenated germanium alloys is related to the smaller electronegativity value of Sn in relation to Ge. However, it can be noted, from Figs. 5 and 6, that Si-H and Si-H₂ stretching modes from $a\text{-Si:H}$ are close to the fitted curve, while in the case of $a\text{-Ge:H}$, the Ge-H and Ge-H₂ the stretching modes are far away from it. The difference between the calculated (ν_{cal}) and experimental (ν_{exp}) stretching frequencies is 136 cm^{-1} for GeH and 62 cm^{-1} for GeH₂. This significant deviation demands an explanation. Some compounds, such as organometallics, silicon, germanium, and tin have vacant d orbitals, whose energy is close to the s - and p -orbital energies of the outer electron shell.²⁹ Therefore these compounds are expected to exhibit conjugation effects such as σ, σ or σ, π . As mentioned earlier, the electronic effect of R^i substituents are responsible for the change in the Ge-H stretching frequency. Thus, the total electronic influence could be separated in the inductive and conjugative effects. Therefore, the higher $\Delta\nu = \nu_{\text{cal}} - \nu_{\text{exp}}$ can be understood if there is a strong contribution of conjuga-

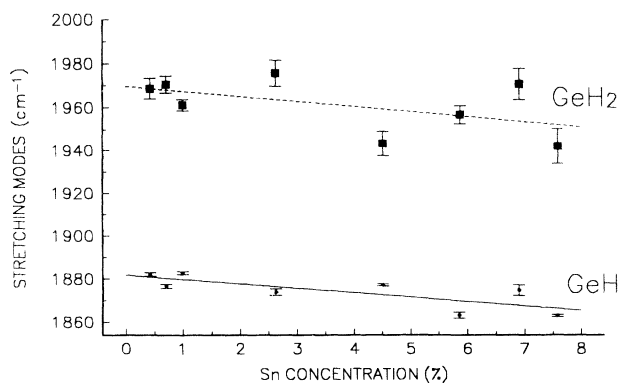


FIG. 4. GeH and GeH₂ stretching mode frequencies vs tin concentration.

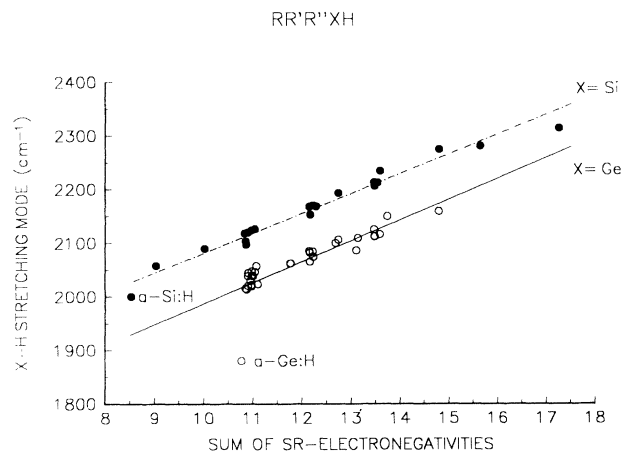


FIG. 5. Frequency of SiH and GeH stretching modes as a function of the sum of the stability ratio electronegativities of the atoms or groups bonded to the Si or Ge atom. The molecular frequencies are from Refs. 24–32.

tive effect in Ge-Ge bond that is much stronger than in Si-Si bond. However, this effect is unlikely because X in $RR'R''XH$ with X and $R^i = \text{Si}$ or Ge , is expected to form four sp^3 tetrahedrally oriented σ bonds and no $(p-d)\pi$ or $(p-d)\sigma$ bonds.³³ In other words, for those compounds $RR'R''\text{GeH}$ and $RR'\text{GeH}_2$ in which the substituents R^i do not form $(p-d)\pi$ or $(p-d)\sigma$ bonds with germanium atom the Ge-H stretching frequency is only inductively influenced. Thus, another explanation must be found.

By using only the inductive mechanism the high $\Delta\nu$ value in $a\text{-Ge:H}$ would be understood if we assume a smaller stability ratio electronegativity value for Ge than the commonly accepted one. This is possible because the electronegativity of germanium relative to the other group-IV elements has been the subject of a great deal of controversy.³³ Using $RR'R''\text{GeH}$ and $RR'\text{GeH}_2$ data the electronegativity average value of Ge in $a\text{-Ge:H}$ is 2.65, which is very close to the electronegativity value of

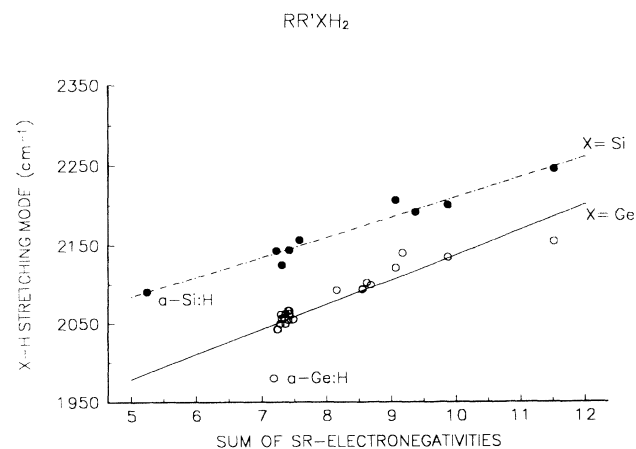


FIG. 6. Frequency of SiH₂ and GeH₂ stretching modes as a function of the sum of the stability ratio electronegativities of the atoms or groups bonded to the Si or Ge atom. The molecular frequency are from Refs. 24–32.

Si (2.62). In order to clarify this point, the $X\text{-H}$ stretching mode of several silicon and germanium compounds (substituted silane and germane, and amorphous) were compared in the Pauling scale. Similar results are expected irrespective of the electronegativity scale. In order to avoid the possible ambiguity of the electronegativity values in some groups, such as CH_3 , C_2H_5 , etc., the empirical equation between Pauling and stability ratio electronegativity scales was not used. Unfortunately, this reduces the amount of data available for the study. However, because similar results in both scales must be obtained, the straight line curves and almost equal slopes for Si and Ge in $RR'R''XH$ systems must be maintained. Figure 7 shows the best fit to the points obtained as just mentioned, giving the following equation in the case of germanium:

$$\omega_{\text{Ge-H}} = 81.5 \left(\sum P^i \right) + 1389.2$$

where $\sum P^i$ is the sum of electronegativities of R^i substituents in Pauling's scale. This result suggests that the stability ratio electronegativity of germanium should be smaller for $a\text{-Ge:H}$ system. Table II shows the Ge-H stretching frequency for the monohydride group in all possible configurations for $R^i = \text{Ge}$ and/or Sn. The shift of the Ge-H modes reflects the different bonding environments provided to the Ge-H bond by the alloyed network, in agreement with Chambouleyron and Marques.¹⁴ However, the Ge-H stretching modes are not noticeably influenced by the masses of the R^i neighbors,²⁴ but by their electronegativities. This can be readily understood since the mass of hydrogen is very light ($m_{\text{H}} = 1.0$) in comparison to that of germanium ($m_{\text{Ge}} = 72.6$) or tin ($m_{\text{Sn}} = 118.7$).

Figure 8 shows the evolution of the GeH wagging frequency and the GeH_2 roll frequency as function of Sn concentration. An increase in the frequency of these two modes is observed as the Sn content increases. This can be explained by a systematic enhancement in the angle-bending force constant for the $R^i\text{-Ge-H}$ bond angle with

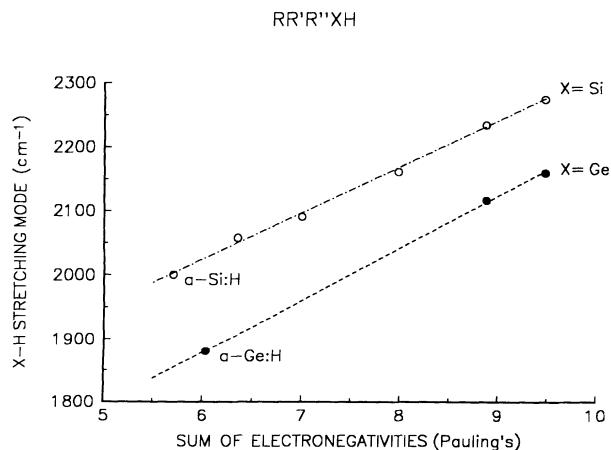


FIG. 7. Frequency of SiH and GeH stretching modes as a function of the sum of Pauling's electronegativities of the atoms bonded to the Si or Ge atom.

TABLE II. Calculated frequency of GeH stretching mode for different R^i configurations.

R^i configuration	Frequency (cm^{-1})
3 Ge	1880.0
2 Ge 1 Sn	1876.5
1 Ge 2 Sn	1872.4
3 Sn	1868.3

increasing Sn concentration, which leads all those motions which involve bond angle distortions to higher frequencies.³⁴ The increase in frequency of the scissors mode in GeH_2 with increasing Sn content is consistent with this explanation. Also, the angular vibrational mode at 890 cm^{-1} in $\text{Si}_{1-x}\text{Sn}_x\text{:H}$ is shifted to 900 cm^{-1} with increasing Sn concentration.^{7,8} The same argument explains the difference in frequency of the GeH wagging ($\sim 565 \text{ cm}^{-1}$) and the GeH_2 roll ($\sim 620 \text{ cm}^{-1}$) modes, where different $R^i\text{-Ge-H}$ bond angles can be formed in the GeH and GeH_2 groups. Several studies have shown that a lower substrate temperature (T_s) is responsible for the occurrence of a higher structural disorder, such as larger bond angle variations,^{35,36} which could lead to a higher wagging roll frequency. Guanhua and Fong-quing³⁷ studied $a\text{-Ge:H}$ and $a\text{-GeN}_x\text{:H}$ samples prepared at T_s equal to room temperature, where the wagging-roll band was found to be 625 cm^{-1} , very close to our assigned roll mode. In most of the $a\text{-Ge:H}$ studies, the frequency of the wagging-roll band has been found to be approximately 570 cm^{-1} for higher T_s .^{1,16} This frequency shift, which is associated with a varying structural disorder caused by variation in the preparation condition, is in agreement with our predictions.

B. Raman scattering

The Raman spectra of $a\text{-Ge}$ has been found to be highly sensitive to changes in the structural order, such as bond angle disorder.^{35,36} In particular, experimental evidence has shown that the broadening and the lowering of the frequency of the Ge-Ge TO-like phonon, relative to that observed in $c\text{-Ge}$, is associated with the higher net-

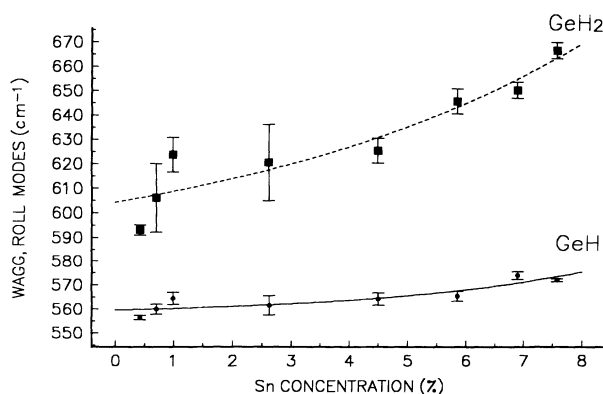


FIG. 8. GeH wagging and GeH_2 roll mode frequencies vs tin concentration.

work structural disorder.³⁵ Moreover, theoretical calculations by Meek³⁸ on models of *a*-Ge with different bond angle distributions and ring statistics have shown that small variations in the short-range order may substantially increase the width of the TO-like phonon band frequency as well as decrease its relative intensity. Figure 9 shows the Raman frequency shift of the Ge-Ge TO-like mode as a function of Sn contents. It is observed to decrease as Sn concentration increases. The covalent radii of Ge and Sn are 0.122 and 0.141 nm, respectively, so that the decreasing of the Ge-Ge TO-like frequency can be explained in terms of the average nearest-neighbor separation, which should increase significantly as Sn is added to the *a*-Ge:H system. Therefore, the increase in Ge-Ge bond length must result in a decrease in the Ge-Ge TO-like frequency. In addition, the incorporated hydrogen should also be partly responsible for this frequency shift. Furthermore, it can be noted, from Fig. 9, that the study with the yellow excitation laser line (2.1 eV), clearly indicates a systematically lower frequency in comparison with that using green laser line (2.4 eV). This can be associated with different absorption depth for yellow and green light photons.^{39,40} In the case of green light, the film layer adjacent to the surface is observed, while with yellow light the scattering from the bulk is measured.

The Ge-Ge TO mode in crystalline germanium is 301 cm^{-1} and it is around 278 cm^{-1} for *a*-Ge:H.^{5,23} Examining Fig. 9, particularly for low Sn concentration, the Ge-Ge bond for layers near the surface are less influenced by the Sn content than that in the bulk. However, this result seems contradictory when you consider the amount of tin near the surface in relation to the bulk. A possible explanation can be given by invoking the very low solubility of Sn in Ge, so that the low tin content in the bulk can form Ge-Sn bonds, while near the surface, despite the Sn content being higher, Sn is less substitutional and it exists as surface aggregates. In this picture, the Ge-Ge bonds are more strongly affected by Sn atoms in the bulk than at the surface. Clustering seems to be a strong possibility in this alloy system based on the precipitation of Sn in the presence of hydrogen and Si substrate.¹⁴ In ad-

dition, Sn clusters or precipitates in *a*-Si_{1-x}Sn_x:H have been related to an increase in the refractive index,⁸ which is in agreement with our results (Table I).

Another contribution to the frequency shift of the Ge-Ge TO-like band in the bulk in comparison to that near the surface is through the hydrogen content. Hishikawa *et al.*⁴¹ have found that the presence of hydrogen atoms in the monohydride configurations (H_m) acts like an interstitial impurity in the silicon network, inducing repulsive force between H_m and neighboring silicon atoms, that results in the expansion of the Si-Si bonds and a decrease in the frequency of the Si-Si TO-like mode. As mentioned before, the FTIR spectra showed a reduction of the hydrogen concentration and a preferential formation of monohydride groups with increase in Sn concentration. At the same time, the H_m content is expected to be lowest near the surface; because of tin segregation, the lower Ge content near the surface with respect to the bulk, and a preferential attachment of hydrogen to Ge is expected. Therefore, the expansion in the Ge-Ge bond length should be higher in the bulk than that in the surface, so that a lower Ge-Ge TO frequency in the bulk than that near the surface must be obtained. Extrapolation to $x=0$, in Fig. 9, shows a Ge-Ge TO-like phonon around 266 cm^{-1} for the bulk (yellow light), while near the surface (green light) a Ge-Ge TO-like band around 274 cm^{-1} is found. This indicates, using the hydrogen content explanation, that the concentration monohydride group is noticeably higher in the bulk than near the surface. This result is in agreement with the works of Ghazala, Beyer, and Wagner⁴² and Wagner and Beyer,⁴³ where the monohydride groups are found to be incorporated mainly in the bulk.

Figure 10 presents the full-width at half maxima (FWHM) of the Ge-Ge TO-like band as a function of Sn content. No conclusive differences in FWHM are found for the different excitation laser lines. However, a clear trend toward higher FWHM is observed as tin concentration increases. This tendency can be understood by incorporation of Sn, which increases the local strain around Ge atoms.³⁷ This suggests, similar to the FTIR results,

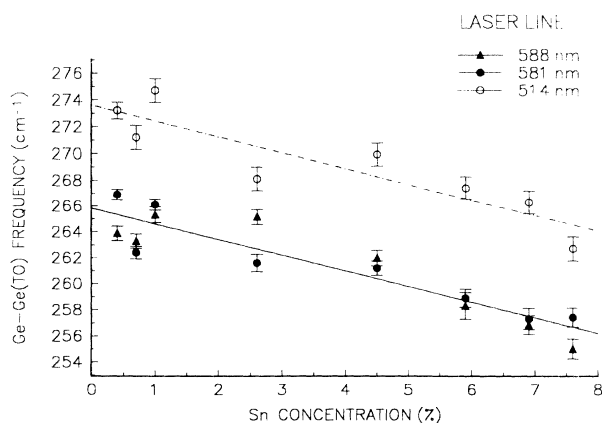


FIG. 9. Frequency of the Ge-Ge TO-like phonon as a function of tin concentration. Different excitation laser lines were used in the Raman-scattering measurements.

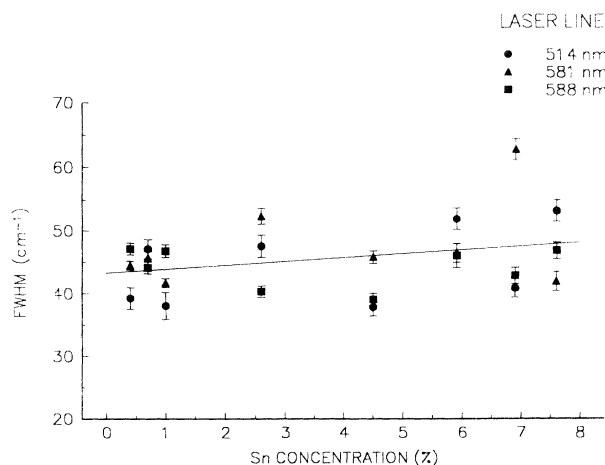


FIG. 10. Full-width at half maxima of the Ge-Ge TO-like mode as a function of tin concentration.

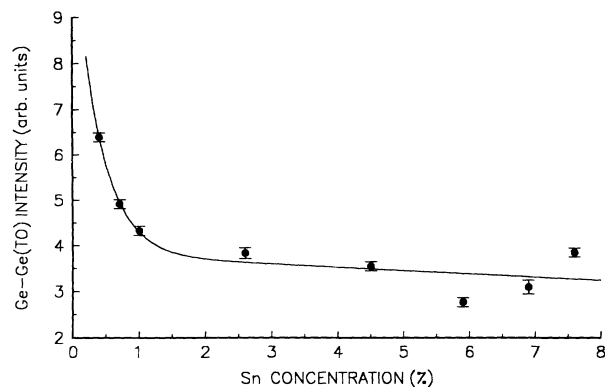


FIG. 11. Intensity of the Ge-Ge TO-like phonon as a function of tin concentration.

that the bond angle deviation increases with increasing tin contents. Using the relationship from the work of Tsu and Hernandez⁴⁴ the angle deviations are between approximately 6° and 12°. Finally, in Fig. 11 we present Ge-Ge TO intensity as a function of Sn concentration. No comparative work was possible for the different excitation laser lines, because for each laser line different defocused spots were used. However, a decrease in the intensity with increasing Sn contents was observed in all cases. Thus, the frequency, the width, as well as the intensity of Ge-Ge TO-like mode, clearly indicate that the structural order decreases with increasing Sn concentration in the α -Ge_{1-x}Sn_x:H system. On the other hand, differences near the surface in comparison to the bulk were observed, which is the product of partial segregation of Sn atoms, formation of Sn clusters, reduction of Ge concentration near the surface and the preferential attachment of hydrogens to Ge than to Sn.

CONCLUSION

We have studied α -Ge_{1-x}Sn_x:H thin films utilizing micro-Raman and infrared spectroscopy techniques. A decrease in hydrogen concentration is found with an increase in Sn concentration. Additionally, a preferential formation of monohydride groups is obtained with increasing Sn concentration. A decrease in the GeH and GeH₂ stretching frequencies with increasing Sn concentration is explained as due to the lower electronegativity of Sn than that of Ge. Also, the study shows that the stability ratio electronegativity should be smaller than 3.59 for the α -Ge:H system. On the other hand, an increase in the GeH wagging and GeH₂ roll frequencies suggests larger bond angle distortion with increasing tin content. The frequency study of Ge-Ge TO-like phonon indicates differences near the surface in comparison to the bulk, which is due to the partial tin segregation and subsequent Sn-clusters formation, the lower germanium concentration near the surface than that in the bulk, and the preferential attachment of hydrogen to Ge than to Sn. Moreover, the halfwidth and intensity of the Ge-Ge TO-like mode shows that the structural disorder increases with increasing Sn content.

ACKNOWLEDGMENTS

The authors thank Dr. Raphael Tsu for helpful comments. They also thank A. Algaze-Beato for his assistance in the FTIR measurements, and G. Morell for critical reading of the manuscript. This work was supported in part by EPSCoR-NSF Grant No. EHR-9108775, and in part by U.S. Army Research Office Grant No. DAAL03-89-G-0114.

- ¹G. Lucovsky, *J. Non-Cryst. Solids* **76**, 173 (1985).
- ²A. Catalano, R. V. D'aiello, J. Dresner, B. Faughnan, A. Firester, J. Kane, H. Schade, Z. E. Smith, G. Swart, and A. Triano, *Proceedings of the 16th IEEE PV Specialists Conference* (IEEE, San Diego, 1982), p. 1421.
- ³A. H. Mahan, D. L. Williamson, and A. Madan, *Appl. Phys. Lett.* **44**, 220 (1984).
- ⁴W. Paul, S. J. Jones, W. A. Turner, and P. Wickboldt, *J. Non-Cryst. Solids* **141**, 271 (1992).
- ⁵D. Bermejo and M. Cardona, *J. Non-Cryst. Solids* **32**, 405 (1979).
- ⁶S. C. Shen, C. J. Fang, and M. Cardona, *Phys. Status Solidi B* **101**, 451 (1980).
- ⁷D. L. Williamson, R. C. Kerns, and S. K. Deb, *J. Appl. Phys.* **55**, 2816 (1984).
- ⁸D. Girginoudi, N. Georgoulas, and A. Thanailakis, *J. Appl. Phys.* **66**, 354 (1989).
- ⁹W. Paul, D. K. Paul, B. V. Roedern, J. Blake, and S. Oguz, *Phys. Rev. Lett.* **46**, 1016 (1981).
- ¹⁰S. Z. Weisz, M. Gomez, J. A. Muir, O. Resto, R. Perez, Y. Goldstein, and B. Abeles, *Appl. Phys. Lett.* **44**, 634 (1984).
- ¹¹R. J. Temkin, G. A. N. Conell, and W. Paul, *Solid State Commun.* **11**, 1591 (1972).
- ¹²S. Oguz and W. Paul, *Appl. Phys. Lett.* **43**, 848 (1983).
- ¹³J. Menéndez, K. Sinha, H. Höchst, and M. A. Engelhardt, *Appl. Phys. Lett.* **57**, 380 (1990).
- ¹⁴I. Chambouleyron and F. C. Marques, *J. Appl. Phys.* **65**, 1591 (1989).
- ¹⁵I. Chambouleyron and F. C. Marques, *J. Appl. Phys.* **63**, 5596 (1988).
- ¹⁶M. Cardona, *Phys. Status Solidi* **118**, 463 (1983).
- ¹⁷R. S. Katiyar, O. Resto, R. Perez, M. Gomez, and Z. Weisz, *Thin Solid Films* **164**, 243 (1988).
- ¹⁸S. Z. Weisz, M. Gomez, J. A. Muir, O. Resto, R. Perez, and Y. Goldstein, *Appl. Phys. Commun.* **4**, 1 (1984).
- ¹⁹M. K. Bhan, L. K. Malhotra, and S. C. Kashyap, *Thin Solid Films* **197**, 269 (1991).
- ²⁰M. H. Brodsky, M. Cardona, and J. J. Cuomo, *Phys. Rev. B* **16**, 3556 (1977).
- ²¹G. A. N. Connell and J. R. Pawlik, *Phys. Rev. B* **13**, 787 (1976).
- ²²G. Lucovsky, R. J. Nemanich, and J. C. Knights, *Phys. Rev. B* **19**, 2064 (1979).
- ²³D. Bermejo and M. Cardona, *J. Non-Cryst. Solids* **32**, 421 (1979).
- ²⁴G. Lucovsky, *Solid State Commun.* **29**, 571 (1979).
- ²⁵R. T. Sanderson, *Chemical Periodicity* (Reinhold, New York, 1960).

- ²⁶J. Janz and Y. Mikawa, *Bull. Chem. Soc. Jpn.* **34**, 1495 (1961).
- ²⁷L. Smith and N. C. Angelotti, *Spectrochim. Acta* **15**, 412 (1959).
- ²⁸A. N. Egorochkin, S. Ya. Khorshev, E. I. Sevastyanova, S. Kh. Ratushnaya, J. Satge, P. Riviere, and J. Barrau, *J. Organomet. Chem.* **155**, 175 (1978).
- ²⁹A. N. Egorochkin, S. Ya. Khorshev, N. S. Ostasheva, J. Satge, P. Riviere, J. Barrau, and M. Massol, *J. Organomet. Chem.* **76**, 29 (1974).
- ³⁰A. N. Egorochkin, S. Ya. Khorshev, E. I. Sevastyanova, S. Kh. Ratushnaya, J. Satge, P. Riviere, J. Barrau, M. Massol, and S. Richelme, *J. Organomet. Chem.* **162**, 25 (1978).
- ³¹J. C. Knights, G. Lucovsky, *CRC Crit. Rev. Solid State Mater. Sci.* **9**, 211 (1980).
- ³²M. Delwaille and M. F. Francois, *C. R. Acad. Sci.* **230**, 743 (1950).
- ³³F. Glockling, *The Chemistry of Germanium* (Academic, London, 1969).
- ³⁴B. K. Ghosh and B. K. Agrawal, *Phys. Rev. B* **33**, 1250 (1986).
- ³⁵J. S. Lannin, L. J. Piloni, S. T. Kshirsagar, R. Messier, and R. C. Ross, *Phys. Rev. B* **26**, 3506 (1982).
- ³⁶M. B. Shubert, H. D. Mohring, R. Zedlitz, and G. H. Bauer, *J. Non-Cryst. Solids* **137&138**, 195 (1991).
- ³⁷C. Guanghua and Z. Fangqing, *Thin Solid Films* **185**, 231 (1990).
- ³⁸E. Meek, in *Proceedings of the Fourth International Conference on the Physics of Non-Crystalline Solids*, edited by G. H. Frischat (Trans. Tech. Aedermansdorf, 1977), p. 586.
- ³⁹G. Morell, R. S. Katiyar, S. Z. Weiz, M. Gomez, and I. Balberg, in *Amorphous Silicon Technology*, edited by E. A. Schiff, M. J. Thompson, A. Madan, T. Tanaka, and P. G. LeComber, MRS Symposia Proceedings No. 297 (Materials Research Society, Pittsburgh, 1993), p. 321.
- ⁴⁰R. Tsu (private communication).
- ⁴¹Y. Hishikawa, K. Watanabe, S. Tsuda, S. Nakano, M. Ohnishi, and Y. Kuwano, *J. Non-Cryst. Solids* **97&98**, 399 (1987).
- ⁴²M. A. Ghazala, W. Beyer, and H. Wagner, *J. Appl. Phys.* **70**, 4540 (1991).
- ⁴³H. Wagner and W. Beyer, *Solid State Commun.* **48**, 585 (1983).
- ⁴⁴R. Tsu and J. G. Hernandez, *J. Non-Cryst. Solids* **66**, 109 (1984).